

Comparison of electron-ion energy transfer in dense plasmas obtained from numerical simulations and quantum kinetic theory

J. Vorberger

Max Planck Institut für die Physik komplexer Systeme, 01187 Dresden, Germany

D.O. Gericke

*Centre for Fusion, Space and Astrophysics, Department of Physics,
University of Warwick, Coventry CV4 7AL, United Kingdom*

(Dated: October 12, 2018)

We evaluate various analytical models for the electron-ion energy transfer and compare the results to data from molecular dynamics (MD) simulations. The models tested includes energy transfer via strong binary collisions, Landau-Spitzer rates with different choices for the cut-off parameters in the Coulomb logarithm, rates based on Fermi's golden rule (FGR) and theories taking coupled collective modes (CM) into account. In search of a model easy to apply, we first analyze different approximations of the FGR energy transfer rate. Then we investigate several numerical studies using MD simulations and try to uncover CM effects in the data obtained. Most MD data published so far show no distinct CM effects and, thus, can be interpreted within a FGR or binary collision approach. We show that this finding is related to the parameter regime, in particular the initial temperature difference, considered in these investigations.

PACS numbers: 52.25.Dg, 52.25.Kn, 52.27.Gr

I. INTRODUCTION

Energy exchange between particles of different species and the subsequent equilibration of their temperatures plays a crucial role in many modern experiments creating high-energy-density matter. A prime example is inertial confinement fusion where intense lasers are employed to heat and compress a deuterium-tritium pellet to extreme conditions [1–4]. Plasmas with well separated electron and ion temperatures are created in the laser spots, the ablator, and the hydrogen pellet itself. In particular, the creation and propagation of the burn wave in the fuel depends on electron-ion temperature equilibration as the main portion of the hydrogen needs to remain cold during compression. Further heating is achieved by α -particles from the hot spot that, however, transfer their energy almost entirely to the electrons. Fusion conditions are thus only reached after sufficient energy transfer from the electronic to the ionic subsystem.

Temperature relaxation is also very important for most experiments dedicated to investigate warm dense matter because a fast energy input into the sample is required to create such a state in the laboratory [5–11]. As the energy is mostly delivered to one species and into special states, samples are often driven into states far from equilibrium. After a short initial equilibration within each species, the system can be characterised by different electron and ion temperatures. Interestingly, ultra-fast probing [12, 13] allows nowadays to investigate dense plasmas on the time scale of temperature equilibration (a few pico-seconds). Even shorter fs-pulses of intense light as delivered by free electron lasers can further increase the time-resolution or may be used to probe the initial relaxation as well [14, 15]. Knowledge of the temperature relaxation time is also important when determining equilibrium properties

like the equation of state or the structure in equilibrium as it sets a minimum time between creation and probing.

As experimental data for the electron-ion equilibration time are sparse, one must often rely on theoretical and simulation results for many applications. The theoretical investigations of electron-ion temperature equilibration can be grouped in two main strains: molecular dynamics (MD) simulations [16, 19–24] and quantum kinetics [25–33]. Both approaches have their strengths and shortcomings: MD simulations are inherently non-perturbative and take into account all channels of energy transfer between the electrons and ions. However, they are based on classical physics for both the electrons and the ions which strongly restricts their range of applicability. Moreover, the use of electron-ion pseudo-potentials designed to mimic aspects of the quantum behaviour raises basic questions.

Quantum statistical theory, on the other hand, is mostly based on perturbation theory with respect to the electron-ion interaction strength. Thus, it offers rates that take into account either strong collisions or energy transfer via collective modes. However, statistical theory can easily account for quantum effects like diffraction and exchange during the scattering process as well as Fermi statistics in degenerate systems.

Here, we conduct an extensive comparison of available MD data with results from quantum statistical theory. First we investigate the electron-ion energy transfer for parameters where strong binary collisions are important. In this connection, we analyze parametrizations of the energy transfer rates in terms of a modified Coulomb logarithm that is chosen to match results of a full binary collision theory (T-matrix approach) [27] or data from MD simulations. Then we evaluate the quality of different approximations often applied when computing of

the energy transfer within the FGR approach and, identify parameter regions where these approximations are applicable. The limits of applicability are particularly important when searching for CM effects by comparing to energy transfer rates based on FGR. Finally, we compare energy transfer rates based on binary collision theory, Fermi's golden rule and the CM approach to results from MD simulations. We find only small hints of CM effects in few of the MD data. The further analysis shows that this finding is related to the small temperature difference considered in most simulations. Moreover, some of the published MD simulations were performed for parameters outside the truly classical regime which may contribute to the inconsistencies found.

II. BINARY COLLISION APPROACH

The electron-ion energy transfer via binary collisions is traditionally described in form of the Landau-Spitzer (LS) approach [34, 35] valid for weakly coupled, classical plasmas. The LS formula for the rate of energy transfer between electrons and ions is expressed in terms of the Coulomb logarithm $\ln \Lambda$

$$Z_{ei} = \frac{k_B (T_i - T_e)}{\left(\frac{k_B T_e}{m_e} + \frac{k_B T_i}{m_i}\right)^{3/2}} \frac{4\sqrt{2}\pi n_e n_i Z_i^2 e^4}{m_e m_i} \ln \Lambda. \quad (1)$$

Here, we have the temperature T_a of species $a = \{e, i\}$, the densities n_a , ion charge state Z_i , the masses m_a , the elementary charge e , and Boltzmann's constant k_B . The Coulomb logarithm contains the information about the strength of the classical two-particle scattering process in the plasma medium and is given by the upper and lower cutoff parameters. The original LS approach, considering straight electron trajectories, yields

$$\ln \Lambda^0 = \ln \frac{b_{max}}{b_{min}}. \quad (2)$$

Many variations for the cutoffs b_{min} and b_{max} have been suggested. More advanced expressions take into account hyperbolic electron orbits in the Coulomb field of the ion and changes to the scattering process due to quantum diffraction effects in close orbits

$$\ln \Lambda^H = \frac{1}{2} \ln \left(1 + \frac{b_{max}^2}{b_{min}^2} \right) = \frac{1}{2} \ln \left(1 + \frac{\lambda_D^2}{\varrho^2 + \lambda_{dB}^2} \right). \quad (3)$$

Here, $\lambda_D = \sqrt{k_B T_e / (4\pi e^2 n_e)}$ is the classical screening (Debye) length, $\varrho = Z_a e^2 / k_B T_e$ denotes the distance of closest approach in the collision, and $\lambda_{dB}^2 = 1 / m_e k_B T_e$ is the deBroglie wavelength defining the range of quantum effects.

One of the shortcomings of the LS approach is that it considers collisions in Coulomb fields and incorporates screening by a cutoff only. Electron-ion collisions in the screened (Debye) potential were considered in the full

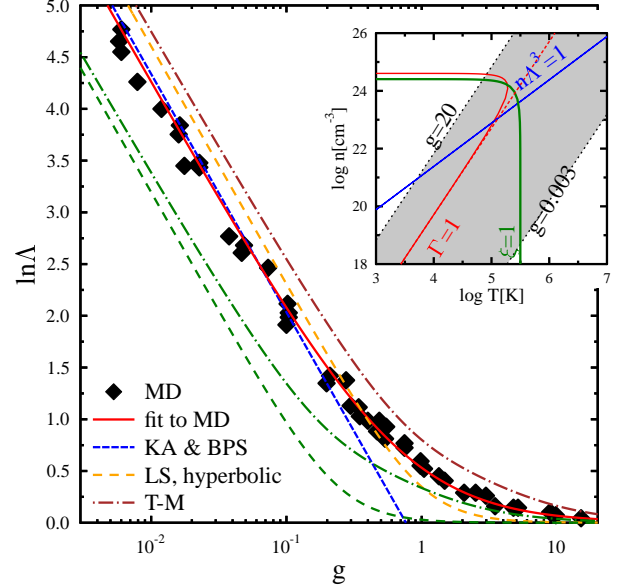


FIG. 1. (color online) Coulomb logarithm for classical systems as derived from MD simulations by Dimonte & Daligault [16] and as predicted by various theories: KA [17], BPS [18]. The results are plotted versus the coupling parameter $g = \varrho / \lambda_D = Ze^2 / (k_B T \lambda_D)$ and for a temperature of $T = 5 \times 10^6$ K. The result from full binary collision theory (brown dash-dotted) and the LS curve (orange dashed) omit the deBroglie wavelength in the minimum cutoff of the Coulomb logarithm as it should be for purely classical systems. The green curves (dash-dotted for TM, dashed for LS) illustrate the effect of the deBroglie wavelength in b_{min} . Quantum effects can be estimated by the parameters $\xi = \varrho / \lambda_{dB}$ and $n\Lambda^3$ (see text).

binary collision approach that is based on the quantum Boltzmann equation [27]. As the collision cross sections were obtained from solutions of the Schrödinger equation [36], quantum diffraction is also fully accounted for. The results were fit to the form (3), using the upper cutoff as a free parameter

$$\ln \Lambda^{bc} = \frac{1}{2} \ln \left(1 + \frac{b_{up}^2}{\varrho^2 + \lambda_{dB}^2} \right)$$

with

$$b_{up} = \lambda_D \cdot \exp \left\{ \frac{1.65 - 0.4 \cdot \ln \Lambda^H}{(\ln \Lambda^H)^{0.64} + 1} \right\}. \quad (4)$$

We compare the formulae (3) and (4) with Coulomb logarithms extracted from classical MD simulations [16] in Fig. 1. The best fit to the MD data has the same functional form as Eq. (3): $\ln \Lambda \sim \ln(1 + 0.7/g)$. The MD simulations were performed for particles with the same charge which allowed for the application of pure Coulomb interactions (no electron-ion pseudo-potential) in classical dynamics. To be consistent with a classical system

like this, we omit the deBroglie wavelength in the minimum cutoff of the Coulomb logarithm. The results of both Eqs. (3) & (4) are in acceptable agreement with the MD data for small coupling and even reproduce the correct behavior for high values of the coupling constant g (strong interactions) reasonably well. Therefore, these MD data clearly show the effects of strong binary collisions. However, CM effects (intentionally not included in the full binary collision approach above) are not visible.

The effect of quantum diffraction can be estimated by including the deBroglie wavelength in the minimum cut-off. We illustrate this effect with the green curves in Fig. 1. Clearly, the consideration of the deBroglie wavelength considerably reduces the Coulomb logarithm and thus the electron-ion energy transfer rate. The importance of diffraction can be estimated by the Born parameter $\xi = \varrho/\lambda_{dB}$ that compares the deBroglie wavelength with the Landau length, i.e. the mean of the closest approach possible between two particles at a certain temperature. For high temperatures, this parameter is small and diffraction is thus important. For high densities/low temperatures, quantum degeneracy limits the classical description. The parameter $n_e \Lambda_e^3 = n_e (2\pi\hbar^2/m_e k_B T_e)^{3/2}$ relates the thermal wavelength of the electrons to their mean distance. When this parameter approaches unity, the electrons become degenerate prohibiting a classical description. Contours of the Born and degeneracy parameters are shown in the inset of Fig. 1 showing the applicability of classical MD simulations in the density-temperature plane.

III. COLLECTIVE EXCITATIONS

Collective excitations can strongly modify the electron-ion energy transfer rates. To include this effect, one has to go beyond the binary collision approach. Considering longitudinal collective excitations in the electron and ion subsystem and their mutual influence, one arrives at the CM expression for the energy transfer rate [25, 32]

$$Z_{ei}^{CM} = -4\mathcal{V} \int \frac{d\mathbf{k}}{(2\pi)^3} \int_0^\infty \frac{d\omega}{2\pi\hbar} \omega \Delta N \frac{\text{Im}\varepsilon_e(\mathbf{k};\omega) \text{Im}\varepsilon_i(\mathbf{k};\omega)}{|\varepsilon(\mathbf{k};\omega)|^2}. \quad (5)$$

Here, $\Delta N_B = n_B^e(\omega, T_e) - n_B^i(\omega, T_i)$ denotes the difference of Bose functions describing the occupation of electron and ion modes. The coupling between the electron and ion modes is facilitated by the dielectric function of the fully coupled electron-ion system

$$\varepsilon(\mathbf{q};\omega) = 1 - \sum_a V_{aa}(q) \Pi_{aa}^R(\mathbf{q};\omega) \quad (6)$$

expressed by the polarisation function of electrons/ions.

Independent collective excitations in the electron and ion subsystem are described within the FGR approach. It can be obtained from the coupled mode expression (5)

by splitting the full dielectric function in the denominator into a product of electron and ion contributions [25, 32]

$$Z_{ei}^{FGR} = -4\mathcal{V} \int \frac{d\mathbf{k}}{(2\pi)^3} \int_0^\infty \frac{d\omega}{2\pi\hbar} \omega \Delta N \times \text{Im}\varepsilon_e^{-1}(k;\omega) \text{Im}\varepsilon_i^{-1}(k;\omega). \quad (7)$$

Here, $\text{Im}\varepsilon_{aa}^{-1}$ are the spectral functions of the collective excitation for the species a . The collective excitations are of Bosonic character and, thus, are populated with a Bose distribution n_B^a for different temperatures T_a .

The FGR expression (7) can be evaluated numerically. However, one would like to avoid the double integration for many applications. This can be achieved using the low ω expansions of the Bose function and the dielectric response of the electrons

$$n_B^a(\omega) \approx \frac{k_B T_a}{\hbar\omega} \quad (8)$$

$$\frac{\text{Im}\varepsilon_e^{-1}}{\omega} \approx \frac{\text{Im}\varepsilon_e^{-1}}{\omega} \Big|_{\omega=0} = C(k) \quad (9)$$

which allows to perform the ω -integral using the f-sum rule for the ions [26]. The approximations above are often applicable due to the separation of the electron and ion excitations in energy space. Moreover, the ion response function effectively limits the ω -integral in the energy transfer rate to small frequencies.

For the electron-ion energy transfer rate, we arrive at

$$Z_{ei}^{(1)} = k_B(T_i - T_e) \frac{4\pi Z_i^2 e^2 n_i}{m_i} \int \frac{d\mathbf{k}}{(2\pi)^3} \frac{\text{Im}\varepsilon_{ee}^{-1}(k,\omega)}{\omega} \Big|_{\omega=0}. \quad (10)$$

For arbitrary degeneracy, one can express the electron dielectric function in the low frequency limit by static screening and the Fermi distribution for the electrons. Then one obtains

$$Z_{ei}^{(2)} = k_B(T_i - T_e) \frac{4Z_i e^4 n_e m_e^2}{\pi m_i} \int_0^\infty dk \frac{k^3}{(k^2 + \kappa_e^2)^2} f_e\left(\frac{k}{2}, \mu\right). \quad (11)$$

The screening parameter κ_e is calculated via

$$\kappa_e^2 = \frac{4\pi e^2}{m_e k_B T_e \Lambda_e^3} I_{1/2}(\beta\mu_e), \quad (12)$$

where $\Lambda_e = \sqrt{2\pi\hbar^2/m_e k_B T_e}$ is the electron's thermal wavelength and $I_{1/2}$ is the Fermi integral of order 1/2.

In the limit of low electron degeneracy, the screening length becomes the Debye length and the Fermi function a Boltzmann distribution. Then the energy transfer rate simplifies to

$$Z_{ei}^{(3)} = k_B(T_i - T_e) \frac{16\sqrt{\pi m_e} n_e^2 Z_i e^4}{m_i (2k_B T_e)^{3/2}} \times \{e^a \text{Ei}(a) - 1 + e^a a \text{Ei}(a)\}, \quad (13)$$

with $a = \lambda_{dB}^2 \kappa_e^2 / 8$ and

$$\text{Ei}(x) = \int_x^\infty ds \frac{e^{-s}}{s}. \quad (14)$$

For highly degenerate systems, we get from a Sommerfeld expansion of the electron distribution function

$$\begin{aligned} Z_{ei}^{(4)} = k_B(T_i - T_e) \frac{4n_e Z_i e^4 m_e^2}{\pi m_i} \\ \times \left\{ \frac{1}{2} \left[\ln(4\mu_e + \kappa_e^2) + \frac{\kappa_e^2}{4\mu_e + \kappa_e^2} - \ln(\kappa_e^2) - 1 \right] \right. \\ \left. + \frac{\pi^2 k_B^2 T_e^2}{6} \left[\frac{12\mu_e}{(4\mu_e + \kappa_e^2)^2} - \frac{64\mu_e^2}{(4\mu_e + \kappa_e^2)^3} \right] \right\}. \end{aligned} \quad (15)$$

In this case, the chemical potential μ is the Fermi energy of the electrons.

Figure 2 compares the different approximation of the FGR energy transfer rate, i.e., Eqs. (11), (13), and (15) with the full FGR expression (7). Clearly, the reduced expression of the FGR approach (13) works very well for non-degenerate systems. Here, the expansion of the Bose function is valid. Thus, the simple expression (13) can be used for all cases with $T_e > T_i$ and nondegenerate electrons. The reduced expression (11), valid for arbitrary electron degeneracy, extends the range of the reduced formula slightly towards smaller electron temperatures.

However, the situation dramatically changes for cases where the electron temperature is smaller than the ion temperature. Here, the full FGR formula (7) predicts energy transfer rates that differ up to a factor of two from the results of the reduced models. These deviations become more pronounced with higher density and the full and reduced models show a qualitatively different behavior for the highest density shown. The main source of deviation is the expansion of the Bose functions $n_a^B(\omega)$ used to derive the reduced models. As soon as the energy of the ion modes becomes comparable to the thermal energy of the electrons, $k_B T_e$, this expansion becomes invalid. As the first order expansion of the Bose functions is at the heart of all reduced descriptions, one has to solve the full FGR expression (11) for all cases with $T_e < T_i$ or degenerate electrons to get valid energy transfer rates. It should be mentioned that the $T=0$ expansion used to derive the formula (15) is of course valid for low electron temperatures. However, expression (15) only approaches the reduced description (11) in this case and not the results from the full FGR description.

IV. COMPARISON OF ENERGY TRANSFER FROM CM AND FGR WITH MD DATA

In the literature, different quantities are applied to quantify the electron-ion energy transfer in two-temperature systems: energy transfer rates, relaxation

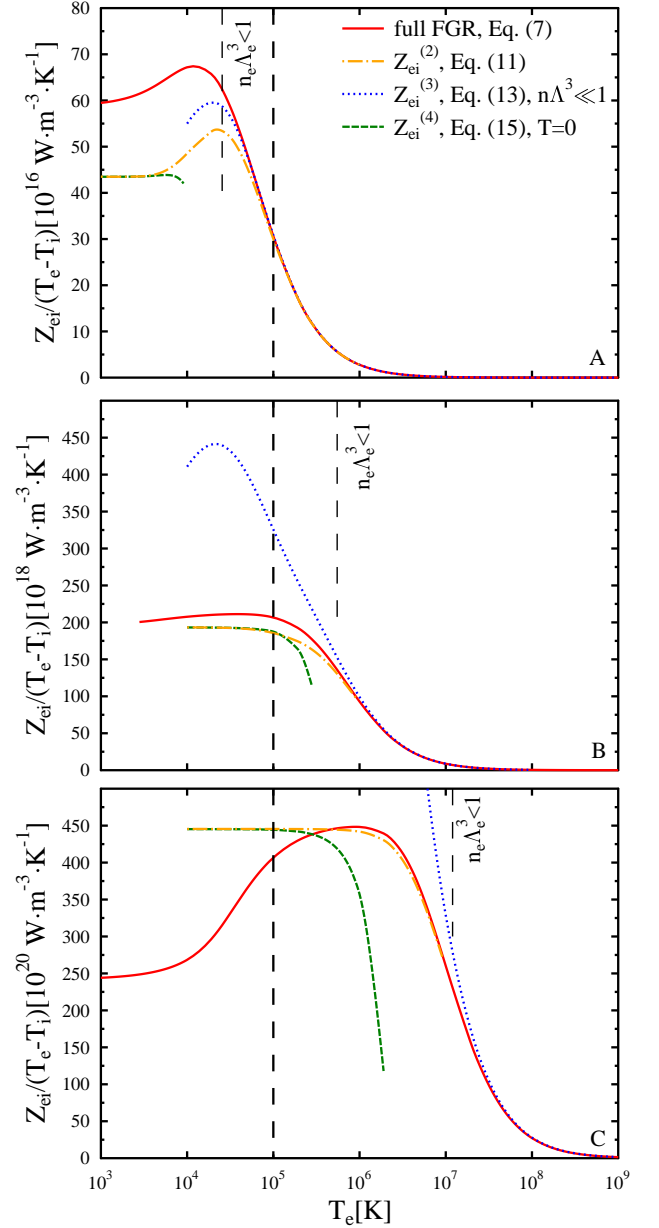


FIG. 2. (color online) Electron-ion energy transfer rates for a fully ionised hydrogen plasma in different approximation levels within the FGR description versus electron temperature. The plasma densities are: $n_e = 10^{22} \text{ cm}^{-3}$ for panel A, $n_e = 10^{24} \text{ cm}^{-3}$ for panel B, and $n_e = 10^{26} \text{ cm}^{-3}$ for panel C. The thick dashed vertical line labels the ion temperature of $T_i = 10^5 \text{ K}$. The thin dashed line indicates where the degeneracy parameter $n_e \Lambda_e^3$ is unity. Left of this line the electrons are fully degenerate.

times, and coupling constants. Most measures eliminate the temperature difference, $T_e - T_i$, to allow for a more unified description although the temperature difference might not be explicitly visible as in the LS case.

To compare with data from MD simulations, we define

TABLE I. Electron-ion coupling parameter for cases A-D of Ref. [19] by Jeon *et al.*: $n_e = n_i = 2.4 \times 10^{22} \text{ cm}^{-3}$, $T_e = 80 \text{ eV}$, $T_i = 100 \text{ eV}$ for case A; $n_e = n_i = 2.68 \times 10^{23} \text{ cm}^{-3}$, $T_e = 400 \text{ eV}$, $T_i = 500 \text{ eV}$ for case B; $n_e = n_i = 7.59 \times 10^{23} \text{ cm}^{-3}$, $T_e = 800 \text{ eV}$, $T_i = 1000 \text{ eV}$ for case C; $n_e = n_i = 2.4 \times 10^{25} \text{ cm}^{-3}$, $T_e = 8000 \text{ eV}$, $T_i = 10000 \text{ eV}$ for case D. The data for MD, MFGR_{AA}, MFGR_C, BPS, and LS⁰ are taken from Ref. [19]. Results labelled LS^H were calculated from Eq. (3) and TM labels data of the fit to the full binary collision approach obtained by Eq. (4). FGR results were obtained from the full FGR expression (7) and are identical to results from the CM approach for the conditions presented here. Data labelled MD^{DD} are based on the Coulomb logarithm given by Dimonte & Daligault [16]. The results for all cases are ordered by value.

case	$g_{ei} [\text{W/m}^3/\text{K}]$								
$(\xi = R_c/\lambda_{dB})$	method								
A $\times 10^{17}$	0.88	0.90	1.03	1.31	1.42	1.51	1.52	1.53	1.57
(0.58)	MFGR _{AA}	LS ⁰	MD	LS ^H	TM	MD^{DD}	FGR	BPS	MFGR _C
B $\times 10^{18}$	0.98	1.24	1.40	1.76	1.77	1.91	1.93	1.94	2.41
(0.26)	MD	LS ⁰	MFGR _{AA}	LS ^H	TM	MFGR _C	FGR	BPS	MD^{DD}
C $\times 10^{18}$	3.81	4.06	4.62	5.30	5.65	5.75	5.79	5.81	7.66
(0.18)	LS ⁰	MD	MFGR _{AA}	LS ^H	TM	FGR	BPS	MFGR _C	MD^{DD}
D $\times 10^{20}$	1.51		1.74	1.99	2.08	2.10	2.13	2.14	3.30
(0.06)	LS ⁰	–	MFGR _{AA}	LS ^H	TM	FGR	MFGR _C	BPS	MD^{DD}

the electron-ion coupling parameter g_{ei}

$$g_{ei} = g^x = \frac{Z_{ei}^x}{T_e - T_i}, \quad (16)$$

the arbitrary Coulomb logarithm

$$\ln \Lambda^x = \frac{Z_{ei}^x}{T_e - T_i} \frac{m_e m_i}{4\sqrt{2\pi n_e n_i} Z_i^2 e^4 k_B} \left(\frac{k_B T_e}{m_e} + \frac{k_B T_i}{m_i} \right)^{3/2}, \quad (17)$$

and the relaxation time

$$\tau^x = k_B (T_e - T_i) n_e \frac{1}{Z_{ei}^x} = \frac{k_B n_e}{g_{ei}}. \quad (18)$$

The label ‘x’ denotes here the approximation level used. All three quantities can be on the level of the full binary collision (T-matrix) approach, the FGR expression, or the full CM description depending on the energy transfer rate Z_{ei} applied as input.

We first compare data from MD simulations to two-temperature models employing various energy transfer rates for cases with low degeneracy. Jeon *et al.* provided just such data [19]. For comparison, we add results of our statistical models (FGR, CM) and from classical MD simulation of Dimonte and Daligault [16] in Fig. 3 and Table I. The densities and temperatures as chosen by Jeon *et al.* correspond to nearly identical parameters of coupling and degeneracy. On this basis, one would not expect qualitative changes in the relaxation behavior between the different cases presented. Indeed, the energy transfer rates on the level of the CM, TM, FGR, BPS, and hyperbolic LS approaches show all a quite regular behavior: these rates keep the same order with respect to the efficiency of the energy transfer and give consistently a higher energy transfer than the MD simulations. The reduced FGR energy transfer rates MFGR_{AA} as given by

Jeon *et al.* are found however to be smaller than MD for case A and larger than MD data for case B and C. The modified FGR approach, MFGR_C of Jeon *et al.*, matches the full FGR formula (blue curves in Fig. 3).

Interestingly, the simplest approximation to the Landau-Spitzer formula (2), LS⁰, using the Debye length for the upper cutoff b_{max} and the deBroglie wavelength for the lower cutoff b_{min} gives best agreement with the MD data for all cases. This might be related to a compensation of errors. Such a result is even more surprising as the full FGR and TM rates incorporating Boltzmann statistics should be the best approximations in cases A to D.

However, one observes that the Born parameter is smaller than unity, $\xi < 1$, and decreases further from case A to D. This fact indicates that the individual two-particle scattering process has significant quantum diffraction effects if it involves electrons and, thus, should be described quantum-mechanically. Diffraction effects are approximated in the MD simulations of Jeon *et al.* by using an electron-ion pseudo-potential of the Deutsch type [19].

One may study the influence of the effective potential on the relaxation by comparing with MD data obtained without the use of a pseudo-potential, e.g., by simulating like-charges of different masses. Table I contains such MD results as obtained by Dimonte & Daligault [16] in addition to the analytical results. One observes that the difference between the data from the two different MD simulations increases from cases A to D. Moreover, the results from MD simulations without pseudo-potential [16] compare quite well to analytical theories in case A where diffraction effects have the least influence. For lower values of the Born parameter, indicating situations with stronger diffraction effects, quantum approaches show significantly less energy transfer in agreement with the

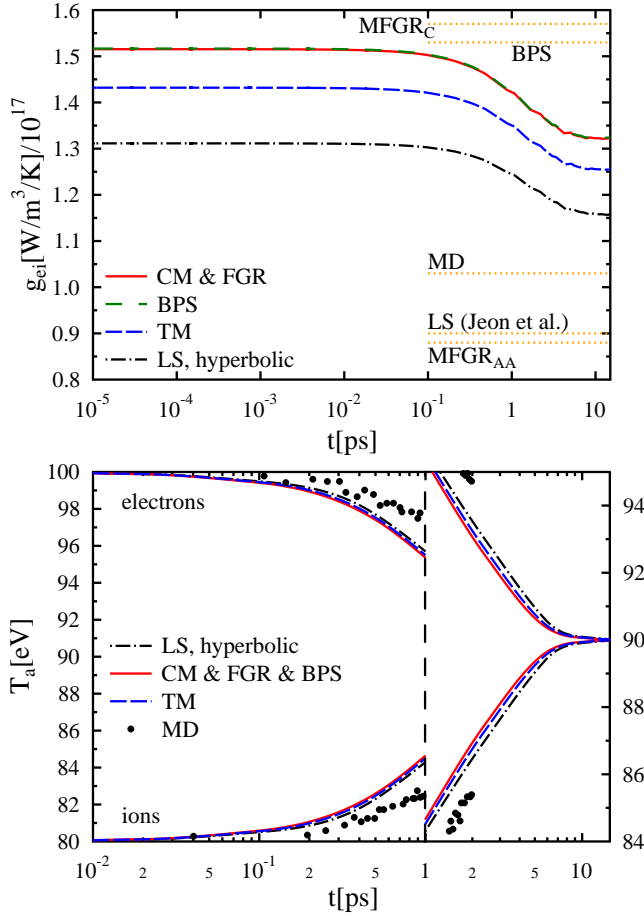


FIG. 3. (color online) Temperature relaxation and energy transfer rates in hydrogen for the case A as studied with MD in Jeon *et al.* [19]. The plasma parameters are $n_e = n_i = 2.4 \times 10^{22} \text{ cm}^{-3}$, $T_e = 80 \text{ eV}$, and $T_i = 100 \text{ eV}$. The straight lines in the upper panel are the values as given in Ref. [19]. *Beware the change in scale of the y-axis at 1ps in the bottom panel.*

findings of Fig. 1. This comparison indicates that the application of the Deutsch potential overestimates the effects of quantum diffraction. Thus, simulations using this potential underestimate the temperature relaxation rates for these parameters.

For high-density plasmas with lower temperatures, quantum (Fermi) statistics and collective effects play a crucial role in the energy transfer process. Therefore, CM and FGR energy transfer rates have been applied to adequately describe the physics processes involved. It is demonstrated in Figs. 4 and 5 how a description of energy transfer by MD compares against these theories in situations where the electrons are close to being degenerate.

For the two cases with lower density shown in Fig. 4, there is virtually no difference between FGR, CM, and BPS results. All these theories predict effective Coulomb logarithms on the upper end of error bars of the data from the MD simulations. Binary collision approaches to the

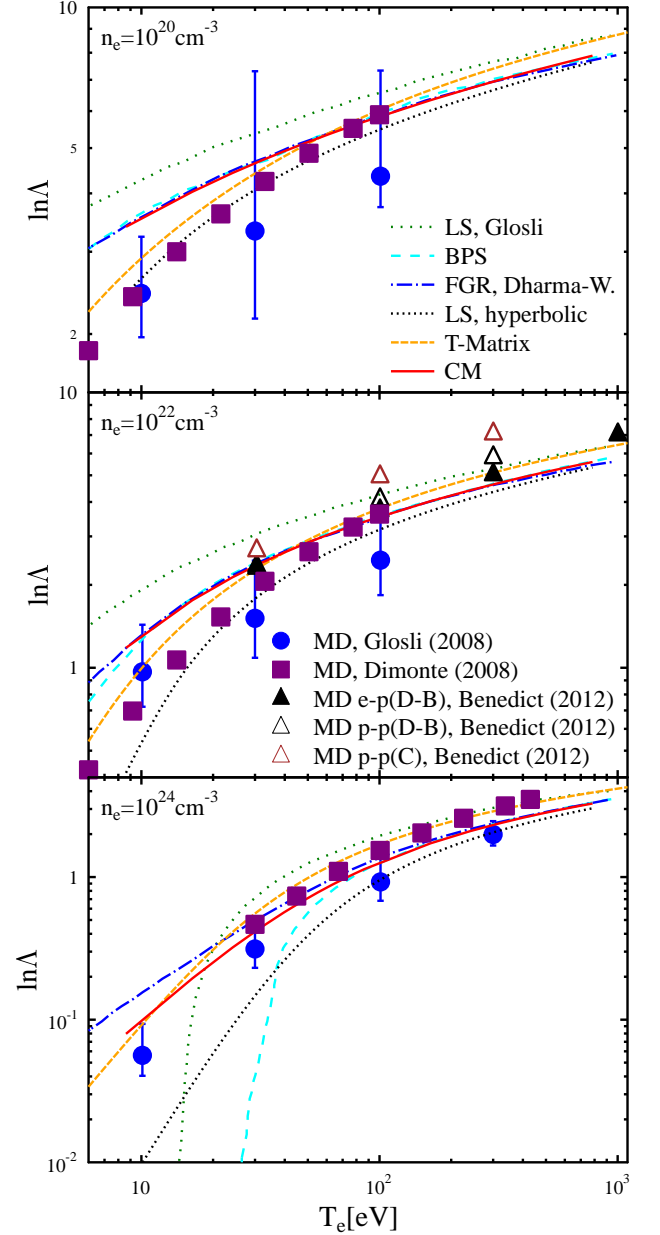


FIG. 4. (color online) Effective Coulomb logarithm as derived from MD simulations by Glosli *et al.* [20] and extracted from various other theoretical schemes for hydrogen at various electron densities. The ion temperature is always twice as high as the electron temperature. These cases correspond to Tab. I and Fig. 2 of Ref. [20]. The purple squares indicate the Coulomb logarithms from a fit to classical MD simulations by Dimonte & Daligault [16]. The triangles are data from Benedict *et al.* [24]

electron-ion energy transfer, namely the parametrized T-matrix model [27] and the LS model featuring hyperbolic orbits, show however much better agreement with the MD data for $n_e = 10^{20} \text{ cm}^{-3}$ and $n_e = 10^{22} \text{ cm}^{-3}$. This fact may indicate that strong scattering as included in the full binary collision approach [27] and approximated

by the LS results is important for these cases. Typically, the Born approximation as used by the FGR and CM theories overestimates the strength of the interaction.

The data by Glosli *et al.* [20] lie also in the area of validity for the MD results by Dimonte & Daligault [16]. Results of the fit given by Dimonte & Daligault and the Coulomb logarithms extracted by Glosli *et al.* show good agreement for low electron temperatures but deviations (still within the error bars given) from 30 eV to 100 eV where quantum diffraction effects may become more important. The results from the fit to MD data of Dimonte & Daligault follow the full binary collision approach and hyperbolic LS results more closely as found earlier.

New extensive MD simulations by Benedict *et al.* [24] for $n_e = 10^{22} \text{cm}^{-3}$ show the best agreement with T-matrix results of all MD simulations if a Dunn&Broyles electron-ion pseudopotential is used. When changing the pseudopotential and the substitution of electrons by positrons, the Coulomb logarithm obtained from the simulations increases and the agreement with other approaches worsens (see middle panel of Fig. 4). The full quantum scattering theory beyond the Born approximation gives, however, also different cross sections if the scattering of like charges is considered. Thus, one may also expect different energy transfer rates.

For the highest density presented in the lower panel of Fig. 4, all variations of the LS formula as well as the BPS model break down at lower temperatures due to the high degree of degeneracy. Differences between the FGR approach (as calculated by Dharma-wardana [29]) and our CM energy transfer rate begin to show due to the occurrence of degeneracy driven ion acoustic modes and thus CM effects [31]. In this case, the CM approach agrees slightly better with the MD data. Again MD simulations of Dimonte & Daligault avoiding electron-ion pseudo-potentials with like-charges yield higher effective Coulomb logarithms and, therefore, higher energy transfer rates. However, one has to point out that classical MD simulations become questionable for high-density systems with high degeneracy.

Fig. 5 summarizes results for the relaxation time, as defined in Ref. [21] and Eq. (18), for a hydrogen plasma at even higher densities. The results from all approaches, analytical theories and numerical simulations, converge for high electron temperatures but differ strongly for lower temperatures. In contrast to the findings in Fig. 3, the LS approximation using straight line trajectories and simple cut-off parameters differs the most from the MD data whereas the LS model using hyperbolic orbits (3) matches the MD data points remarkably well (except after the break-down at low electron temperatures). Results from FGR models always fare worse than CM results when compared to the MD data.

The parameters investigated in Fig. 5 are one of the few cases where systems with an ion temperature well below the electron temperature have been studied by MD simulations. Under these conditions, coupled collective modes exist [31] and a deviation of the CM rates from

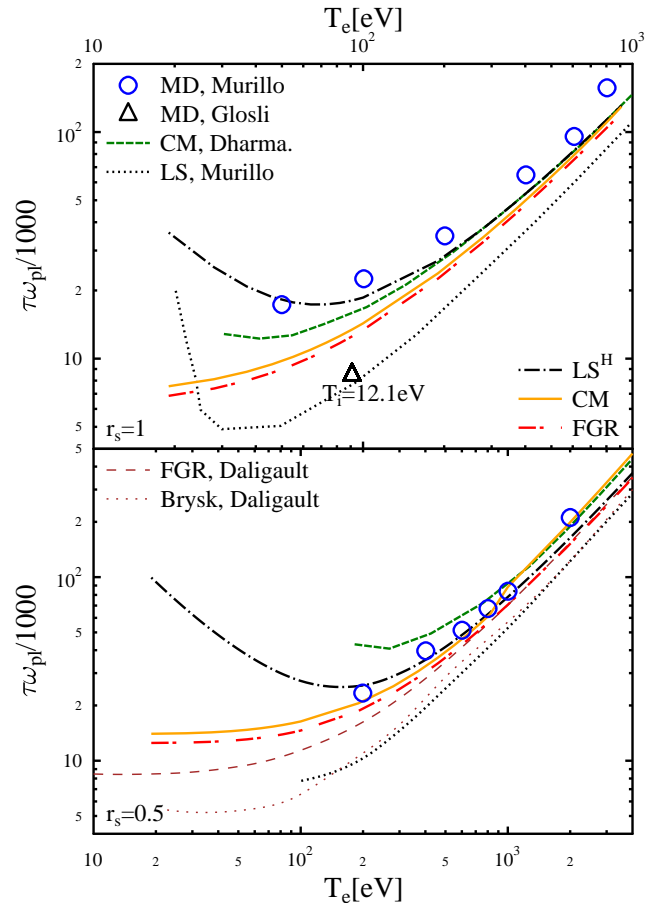


FIG. 5. (color online) Relaxation times obtained from MD simulations for the cases studied by Murillo & Dharma-wardana [21], Glosli *et al.* [20], and Daligault & Dimonte *et al.* [23] for a hydrogen plasmas compared to results from different versions of the LS, FGR, and CM approaches. The ion temperature is $T_i = 10$ eV except for the data point from Glosli *et al.*

FGR rates can indeed be observed. This coupled mode effect is even visible for the highest temperatures at $r_s = 0.5$. Here, the rates from the CM expression agree with MD results and give a systematically different limit as theories not including CM effects. Indeed, the CM theory yields approximately 30% longer relaxation times than FGR or LS formulas predict.

V. SUMMARY AND CONCLUSION

We have compared data for the relaxation of two-temperature electron-ion systems obtained by classical MD simulations with predictions of different analytical approaches. For our extensive comparison, we considered i) theories treating binary collisions only (the simple LS formula and the full binary collision (T-matrix) approach [27]) and ii) theories considering collective excitations in the plasma (FGR and CM expressions [25]). Our

main goals were to benchmark the quality of collisional models against MD simulations and to search for indications of coupled mode effects in the MD data. The latter should be possible as MD simulations not only compute the classical collision processes but also cover the classical dynamics and collective motions in full which in certain parameter regimes gives rise to energy transfer via collective modes - the CM effect.

Our comparisons of MD data and theories considering binary collisions only showed the well-known inability of the simple LS approach (considering straight line trajectories) to predict the electron-ion energy transfer. The LS expression for hyperbolic orbits with appropriate cutoffs as well as the fit to the full binary collision (T-matrix) approach [27] yield however satisfying agreement with the MD data obtained by Dimonte & Daligault [16] if applied to classical plasmas. We have chosen this set of MD data here as the underlying simulations were performed for like-charges interacting with bare Coulomb forces. Thus, these MD data contain no uncertainty related to the electron-ion pseudo-potential.

In the search of CM effects, one should always compare MD data with the FGR and CM expressions since the LS formula yields energy transfer rates and relaxation times that may strongly depend on the cutoffs used. Therefore, deviations between MD data and LS results are more likely related to a failure of the LS approach than a hint of CM effects. To avoid false indications, we have also investigated the validity of various approximations and simplifications to the FGR expression. We found that for many cases, in particular for low electron temperatures, none of the reduced FGR expressions are applicable as they are all based on the expansion of the Bose function which becomes invalid. Thus, we have evaluated the full FGR expression (7) to make unambiguous comparisons with the MD data.

Most MD simulations were performed for parameters where the condition for the occurrence of ion acoustic modes in classical plasmas, i.e. $ZT_e \gg T_i$, is not fulfilled. Accordingly, the data for the electron-ion energy transfer show negligible influence of coupled collective modes. For cases with low degeneracy where such classical simulations are applicable, full T-Matrix and hyperbolic LS rates compare best to MD as expected. If the electron-ion coupling is also weak, full FGR and CM rates agree as well. For systems with degenerate electrons, neither MD simulations nor the discussed binary collision approaches are applicable and one has, so far, to rely on the comparison of FGR and CM rates when searching for CM effects.

However, the MD data published in Ref. [21] fulfill the condition for the occurrence of coupled electron-ion modes as the electron temperature exceeds the ion temperature several times. As discussed in connection with Fig. 5, the temperature relaxation times differ significantly whether or not the theoretical approach includes coupled collective modes and the results from the full CM description agree best with MD data. Interestingly,

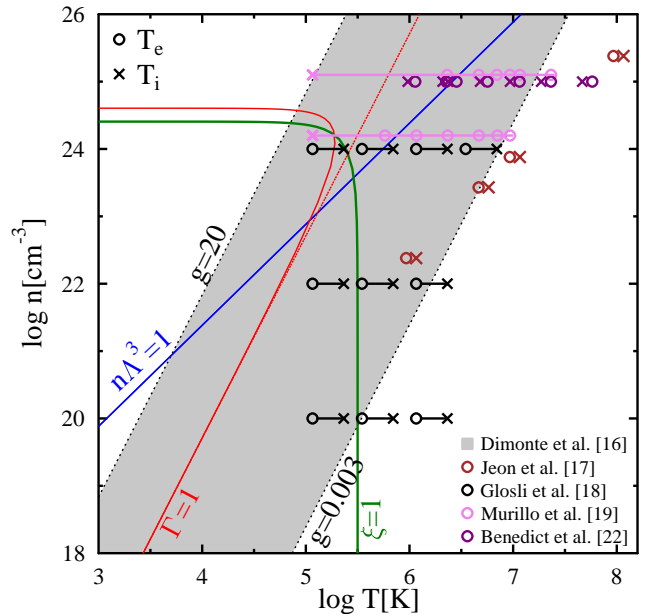


FIG. 6. (color online) Plasma parameters considered in recent MD simulations investigating electron-ion temperature relaxation in relation to the degeneracy parameter $n_e \Lambda_e^3$ with $\Lambda_e = (2\pi/m_e k_B T)^{1/2}$, the classical coupling parameter $\Gamma = \rho/d \sim \langle K \rangle / \langle V \rangle$ with $d = (3/4\pi n)^{1/3}$, and the Born parameter $\xi = \rho/\lambda_{dB}$. Above the degeneracy line $n_e \Lambda_e^3 = 1$, the electrons are highly degenerate; to the right and the top of the curve $\xi = 1$, quantum diffractions become important for the two-particle scattering process. The grey area marks parameters considered in Ref. [16].

this relation holds even for very high electron temperatures as predicted before [31] within the weak coupling CM approach. This finding is a strong indication for CM effects in the relaxation time data extracted from MD simulations. A remaining source of uncertainty is the use of electron-ion pseudo-potentials in the MD simulations. A possible overcompensation of quantum diffraction by the effective potential will result in a reduction of the electron-ion energy transfer and, thus, might mimic CM effects.

It has been shown that some MD simulations show strong signs of CM effects on temperature relaxation. However, MD data must be interpreted with care as these classical simulations do not include quantum effects. Of course, the ions are well described by Newton's equations but the electronic subsystem can exhibit both quantum degeneracy at high densities and diffraction effects during high-energy collisions dominating at high temperatures. The importance of quantum effects can be estimated by the degeneracy parameter $n_e \Lambda_e^3$ and the Born parameter ξ , respectively.

In Fig. 6, the plasma parameters of MD simulations considering two-temperature electron-ion systems have been plotted together with contours of the degeneracy,

coupling, and Born parameters. Systems above the line $n_e\Lambda_e^3 = 1$ are plagued by quantum degeneracy while points on the right side of the line $\xi = 1$ exhibit strong quantum diffraction that is most likely not well described by an electron-ion pseudo-potential. To distinguish CM effects clearly from artifacts of the pseudo-potential, we suggest to perform MD simulations at low densities and temperatures to maintain $n_e\Lambda_e^3 < 1$ and $\xi < 1$. The need of pseudo-potentials can be also strongly mitigated by considering systems with like charges. Moreover, the electrons need to be still much hotter than the ions as CM effects occur only for $T_i \ll T_e$ in classical systems.

Most MD simulations performed so far do not meet all requirements to clearly observe CM mode effects as they often consider systems with $T_i > T_e$. Comparing the MD data with both results from a full CM theory

and the FGR approach, one finds strong indications of CM effects in the few MD data for $T_i < T_e$. However, these simulations are too close, or even beyond, the lines $n_e\Lambda_e^3 < 1$ or $\xi < 1$ to unambiguously exclude that the reductions in energy transfer observed are related to the application of pseudo-potentials or the break of classical statistics inherent to MD simulations.

VI. ACKNOWLEDGEMENTS

The authors thank the UK's Engineering and Physical Sciences Research Council for financial support of this work.

-
- [1] J.D. Lindl *et al.*, Phys. Plasmas **11**, 339 (2004).
 - [2] S.H. Glenzer *et al.*, Science **327**, 1228 (2010).
 - [3] B. Xu and S. X. Hu, Phys. Rev. E **84**, 016408 (2011).
 - [4] J.L. Kline *et al.*, Phys. Rev. Lett. **106**, 085003 (2011); S.H. Glenzer *et al.*, Phys. Rev. Lett. **106**, 085004 (2011); T. Döppner *et al.*, Phys. Rev. Lett. **108**, 135006 (2012); H.F. Robey *et al.*, Phys. Rev. Lett. **108**, 215004 (2012); A.J. Mackinnon *et al.*, Phys. Rev. Lett. **108**, 215005 (2012);
 - [5] A. Ng, P. Celliers, G. Xu, A. Forsman, Phys. Rev. E **52**, 4299 (1995).
 - [6] D. Riley, N.C. Woolsey, D. McSherry, I. Weaver, A. Djaoui, E. Nardi, Phys. Rev. Lett. **84**, 1704 (2000).
 - [7] A. Lévy *et al.*, Phys. Rev. Lett. **108**, 055002 (2012).
 - [8] S.H. Glenzer *et al.*, Phys. Rev. Lett. **98**, 065002 (2007).
 - [9] E. Garcia Saiz *et al.*, Nature Phys. **4**, 920 (2008).
 - [10] A. Pelka *et al.*, Phys. Rev. Lett. **105**, 265701 (2010).
 - [11] T. White *et al.*, Scientific Reports **2**, 889 (2012).
 - [12] A.L. Kritcher *et al.*, Science **322**, 69 (2008).
 - [13] B. Barbreil *et al.*, Phys. Rev. Lett. **102**, 165004 (2009).
 - [14] R. R. Fäustlin *et al.*, Phys. Rev. Lett. **104**, 125002 (2010).
 - [15] D.A. Chapman, D.O. Gericke, Phys. Rev. Lett. **107**, 165004 (2011).
 - [16] G. Dimonte and J. Daligault, Phys. Rev. Lett. **101**, 135001 (2008).
 - [17] T. Kihara, O. Aono, J. Phys. Soc. Jap. **18**, 837 (1963).
 - [18] E.M. Lifshitz and L.P. Pitaevskii, *Physical Kinetics*, Elsevier, Butterworth and Heinemann, Oxford, U.K., (2006), p. 193.
 - [19] B. Jeon, M. Foster, J. Colgan, G. Csanak, J. D. Kress, L. A. Collins, and N. Grønbech-Jensen, Phys. Rev. E **78**, 036403 (2008).
 - [20] J. N. Glosli, F. R. Graziani, R. M. More, M. S. Murillo, F. H. Streitz, M. P. Surh, L. X. Benedict, S. Hau-Riege, A. B. Langdon, R. A. London, Phys. Rev. E **78**, 025401(R) (2008).
 - [21] M. S. Murillo, M. W. C. Dharma-wardana, Phys. Rev. Lett. **100**, 205005 (2008).
 - [22] L.X. Benedict *et al.*, Phys. Rev. Lett. **102**, 205004 (2009).
 - [23] J. Daligault, G. Dimonte, Phys. Rev. E **79**, 056403 (2009).
 - [24] L.X. Benedict *et al.*, Phys. Rev. E **86**, 046406 (2012).
 - [25] M. W. C. Dharma-wardana, F. Perrot, Phys. Rev. E **58**, 3705, (1998).
 - [26] G. Hazak, Z. Zinamon, Y. Rosenfeld, M.W.C. Dharma-wardana, Phys. Rev. E **64**, 066411 (2001).
 - [27] D. O. Gericke, M. S. Murillo, M. Schlanges, Phys. Rev. E **65**, 036418 (2002).
 - [28] J. Daligault, D. Mozysky, High Energy Density Physics **4**, 58 (2008).
 - [29] M. W. C. Dharma-wardana, Phys. Rev. Lett. **101**, 035002 (2008).
 - [30] G. Gregori, D. O. Gericke, Europhys. Lett. **83**, 15002 (2008).
 - [31] J. Vorberger, D. O. Gericke, Phys. Plasma **16**, 082702 (2009).
 - [32] J. Vorberger, D. O. Gericke, T. Bornath, M. Schlanges, Phys. Rev. E **81**, 046404 (2010).
 - [33] S. D. Baalrud, Phys. Plasma **19**, 030701 (2012).
 - [34] L.D. Landau, JETP **7**, 203 (1937).
 - [35] L. Spitzer, *Physics of Fully Ionized Gases*, Interscience, N.Y., (1967).
 - [36] D.O. Gericke, S. Kosse, M. Schlanges, and M. Bonitz, Phys. Rev. B **59**, 10639 (1999).